Published for SISSA by Springer

Received: July 11, 2022
Revised: July 29, 2022
Accepted: August 8, 2022
Published: August 30, 2022

Radiative corrections to the forward-backward asymmetry in $e^+e^- \to \pi^+\pi^-$

Gilberto Colangelo,[a] **Martin Hoferichter,**[a] **Joachim Monnard**[a] **and Jacobo Ruiz de Elvira**[a,b]

[a] *Albert Einstein Center for Fundamental Physics, Institute for Theoretical Physics, University of Bern, Sidlerstrasse 5, 3012 Bern, Switzerland*

[b] *Universidad Complutense de Madrid, Facultad de Ciencias Físicas, Departamento de Física Teórica and IPARCOS, Plaza de las Ciencias 1, 28040 Madrid, Spain*

E-mail: gilberto@itp.unibe.ch, hoferichter@itp.unibe.ch, monnard@itp.unibe.ch, jacobore@ucm.es

Abstract: We present a calculation of the C-odd radiative corrections to $e^+e^- \to \pi^+\pi^-$ in a dispersive formalism, concentrating on the leading pion-pole contribution in the virtual box diagrams. In particular, we show how the effect of a general pion vector form factor in the loop integral can be incorporated in a model-independent way and how the cancellation of infrared singularities proceeds in this case. The numerical results, dominated by the infrared enhanced contributions, indicate significant corrections beyond scalar QED, essentially confirming recent findings in generalized vector-meson-dominance models.

Keywords: Chiral Lagrangian, Precision QED

ArXiv ePrint: 2207.03495

https://doi.org/10.1007/JHEP08(2022)295

JHEP08(2022)295

Contents

1 Introduction

The data-driven determination of hadronic vacuum polarization (HVP) is dominated by the 2π channel, which gives about 70% of the HVP contribution to the anomalous magnetic moment of the muon [1]. The consensus number [2–7]

$$a_\mu^{\text{HVP, LO}}\big|_{e^+e^-} = 693.1(4.0) \times 10^{-10} \tag{1.1}$$

for this quantity relies on a set of measurements from SND [8, 9], CMD-2 [10–13], BESIII [14], and CLEO [15] (and, when dispersive constraints are included [4–6, 16, 17], also on space-like data [18, 19]), but is dominated by the precision data sets from BaBar [20, 21] and KLOE [22–25]. Since ref. [1] new data have become available from SND [26], but resolving the tension between BaBar and KLOE requires new measurements at a similar level of precision, as are expected from CMD-3 [27], BaBar [28], BESIII [29], and Belle II [30]. This question has become increasingly urgent in view of recent lattice-QCD results [31–33] challenging the data-driven value (1.1) at least for the intermediate window [34], and critical for the interpretation [35–39] of the 4.2σ tension between experiment [40–44] and Standard-Model theory [1–7, 45–62].

A potential weak point in the analysis concerns the treatment of radiative corrections [28, 63, 64], which are implemented in Monte-Carlo generators relying on scalar QED supplemented by the pion vector form factor (VFF) wherever possible [65], to capture the

JHEP08(2022)295

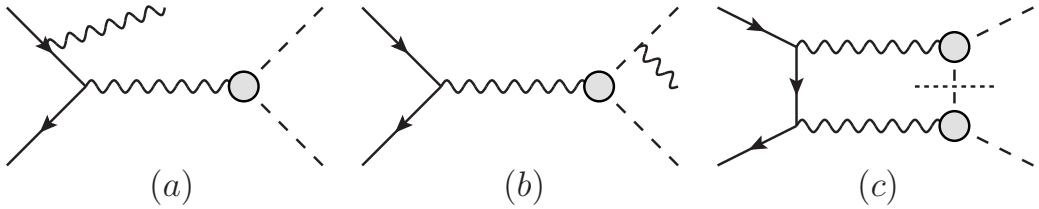

Figure 1. Representative diagrams contributing to $A_{\rm FB}$ (solid, dashed, and wiggly lines denote electrons, pions, and photons, respectively). The interference of ISR (a) and FSR (b) produces real terms odd in z, while box diagrams (c) give the virtual corrections. Only the sum of real and virtual contributions is IR finite. The gray blob denotes the pion VFF, which for (b) can be justified because we only keep the soft limit. The short-dashed line in (c) indicates that we only consider the pion-pole singularities, not general hadronic intermediate states that could contribute to the hadronic side of the box diagram.

dominant corrections from the structure of the pion. In the case of final-state radiation (FSR), this approach does capture the dominant infrared (IR) enhanced effects [66–69], but it is not guaranteed that corrections can be neglected in all kinematic configurations relevant for precision measurements of $e^+e^- \to \pi^+\pi^-$ [70].

A possible test case concerns the forward-backward asymmetry in the same process, in which case radiative corrections arise from the interference of initial-state-radiation (ISR) and FSR diagrams [71–73] combined with box diagrams, see figure 1. While these corrections cancel when integrated over the entire phase space, they can be probed in the forward-backward asymmetry. Writing the Born cross section as

$$\frac{d\sigma_0}{dz} = \frac{\pi\alpha^2\beta^3}{4s}(1-z^2)|F_\pi^V(s)|^2, \qquad \beta = \sqrt{1-\frac{4M_\pi^2}{s}}, \qquad z = \cos\theta, \qquad \alpha = \frac{e^2}{4\pi}, \tag{1.2}$$

with the pion VFF $F_\pi^V(s)$ defined by the matrix element of the electromagnetic current $j^\mu_{\rm em} = (2\bar{u}\gamma^\mu u - \bar{d}\gamma^\mu d - \bar{s}\gamma^\mu s)/3$,

$$\langle\pi^\pm(p')|j^\mu_{\rm em}(0)|\pi^\pm(p)\rangle = \pm(p'+p)^\mu F_\pi^V((p'-p)^2), \tag{1.3}$$

it is clear that the forward-backward asymmetry

$$A_{\rm FB}(z) = \frac{\frac{d\sigma}{dz}(z) - \frac{d\sigma}{dz}(-z)}{\frac{d\sigma}{dz}(z) + \frac{d\sigma}{dz}(-z)} \tag{1.4}$$

vanishes at tree-level, but radiative corrections give rise to odd terms in z. In ref. [74] these corrections were calculated in scalar QED, multiplied in the end globally with $|F_\pi^V|^2$ to account for structure corrections. However, in ref. [75] it was observed that this approximation was insufficient to describe preliminary data from the CMD-3 experiment, proposing an improved approach using generalized vector-meson-dominance (GVMD) models in the loop integral (see ref. [76] for a related analysis).

In this paper, we present a model-independent approach that captures the effect of the pion-pole singularities in the virtual diagrams, and show that the dominant corrections still

JHEP08(2022)295

arise from the IR enhanced effects. For the real contribution, due to the interference of the ISR and FSR diagrams in figure 1, we obtain the correction factor

$$\delta_{\text{soft}} = \frac{2\alpha}{\pi}\left\{\log\frac{\lambda^2}{4\Delta^2}\log\frac{1+\beta z}{1-\beta z} + \log(1-\beta^2)\log\frac{1+\beta z}{1-\beta z} + \log^2(1-\beta z) - \log^2(1+\beta z)\right.$$
$$\left. + \text{Li}_2\left(\frac{(z-1)\beta}{1-\beta}\right) + \text{Li}_2\left(\frac{(1+z)\beta}{1+\beta}\right) - \text{Li}_2\left(\frac{(z+1)\beta}{\beta-1}\right) - \text{Li}_2\left(\frac{(1-z)\beta}{1+\beta}\right)\right\}, \quad (1.5)$$

which agrees with similar representations in refs. [74, 75] and is defined relative to eq. (1.2)

$$\left.\frac{d\sigma}{dz}\right|_{C\text{-odd}} = \frac{d\sigma_0}{dz}\left[\delta_{\text{soft}}(\lambda^2,\Delta) + \delta_{\text{virt}}(\lambda^2)\right] + \left.\frac{d\sigma}{dz}\right|_{\text{hard}}(\Delta). \quad (1.6)$$

The parameter $\lambda = m_\gamma$, a small photon mass, regularizes the IR divergence and Δ is a cutoff in the photon energy (we do not consider the hard contribution with photon energy above Δ any further). As we will show below, already the cancellation of the IR singularity becomes quite subtle for a general pion VFF. After discussing the analytic structure in section 2, we derive our result for the virtual contribution in terms of the standard scalar loop functions in section 3, before turning to the numerical analysis in section 4. Our conclusions are summarized in section 5.

2 Dispersion relations and cut structure

We define the kinematic variables according to

$$e^+(p_2)e^-(p_1) \to \pi^+(l_2)\pi^-(l_1), \quad (2.1)$$

with Mandelstam variables

$$\begin{aligned} s &= (p_1+p_2)^2 = (l_1+l_2)^2, \\ t &= (p_1-l_1)^2 = (p_2-l_2)^2 = \frac{1}{2}\left(2M_\pi^2 + 2m_e^2 - s + z\sigma_e\sigma_\pi s\right), \\ u &= (p_1-l_2)^2 = (p_2-l_1)^2 = \frac{1}{2}\left(2M_\pi^2 + 2m_e^2 - s - z\sigma_e\sigma_\pi s\right), \end{aligned} \quad (2.2)$$

where

$$\sigma_\pi \equiv \beta = \sqrt{1-\frac{4M_\pi^2}{s}}, \qquad \sigma_e = \sqrt{1-\frac{4m_e^2}{s}}, \qquad z = \frac{t-u}{s\sigma_\pi\sigma_e}, \quad (2.3)$$

and $s+t+u = 2M_\pi^2 + 2m_e^2$. In the following, we will always put $m_e = 0$ unless required to regularize collinear singularities.

To isolate the contribution from the pion pole in the hadronic part of the loop diagram, one starts from fixed-s dispersion relations, which for scalar particles would immediately allow one to identify the scalar loop integral D_0 [77] in terms of its double-spectral function. This procedure has been performed in detail for the pion boxes in hadronic light-by-light scattering [78], demonstrating that the non-box contributions that arise in a diagrammatic scalar-QED calculation are simply required by gauge invariance, in such a way that the

JHEP08(2022)295

final result can be obtained by multiplying the scalar-QED amplitude by the appropriate pion VFFs for the external photons.[1]

In the present case a similar argument applies if a dispersive representation is used for the pion VFF in the $e^+e^- \to \pi^+\pi^-$ subamplitudes, i.e., if we replace

$$\frac{F_\pi^V(s)}{s} = \frac{1}{s} + \frac{1}{\pi}\int_{4M_\pi^2}^\infty ds' \frac{\mathrm{Im}\, F_\pi^V(s')}{s'(s'-s)} \to \frac{1}{s-\lambda^2} - \frac{1}{\pi}\int_{4M_\pi^2}^\infty ds' \frac{\mathrm{Im}\, F_\pi^V(s')}{s'}\frac{1}{s-s'} \tag{2.4}$$

for each of the two photon propagators. In eq. (2.4) we have introduced the IR regulator in the pole terms, which are the ones that produce the IR divergence. The resulting representation for the box diagram then consists of pole times pole, mixed pole and dispersive, and dispersive times dispersive contributions. In the next section, we will express each of them in terms of standard loop functions.

3 Formulation in terms of scalar loop functions

The tensor decomposition is easiest to derive directly for the spin sum of the interference of the box diagram with the tree-level amplitude. This gives the decomposition of the virtual correction

$$\begin{aligned}\delta_{\mathrm{virt}} = \bar\delta_{\mathrm{virt}}(\lambda^2,\lambda^2) &- \frac{1}{\pi}\int_{4M_\pi^2}^\infty ds' \frac{\mathrm{Im}\, F_\pi^V(s')}{s'}\left[\bar\delta_{\mathrm{virt}}(s',\lambda^2) + \bar\delta_{\mathrm{virt}}(\lambda^2,s')\right] \\ &+ \frac{1}{\pi}\int_{4M_\pi^2}^\infty ds' \frac{\mathrm{Im}\, F_\pi^V(s')}{s'}\frac{1}{\pi}\int_{4M_\pi^2}^\infty ds'' \frac{\mathrm{Im}\, F_\pi^V(s'')}{s''}\bar\delta_{\mathrm{virt}}(s',s''),\end{aligned} \tag{3.1}$$

with

$$\begin{aligned}\bar\delta_{\mathrm{virt}}(s',s'') = &-\frac{\mathrm{Re}\, F_\pi^V(s)}{2\beta^2 s(1-z^2)|F_\pi^V(s)|^2}\frac{\alpha}{\pi} \\ &\times \mathrm{Re}\Big[4t(M_\pi^2-t)\Big(C_0(m_e^2,t,M_\pi^2,s',m_e^2,M_\pi^2) + C_0(m_e^2,t,M_\pi^2,s'',m_e^2,M_\pi^2)\Big) \\ &\quad - 4u(M_\pi^2-u)\Big(C_0(m_e^2,u,M_\pi^2,s',m_e^2,M_\pi^2) + C_0(m_e^2,u,M_\pi^2,s'',m_e^2,M_\pi^2)\Big) \\ &\quad - 4s(t-u)C_0(m_e^2,s,m_e^2,m_e^2,s',s'') + 4(t^2-u^2)C_0(M_\pi^2,s,M_\pi^2,M_\pi^2,s',s'') \\ &\quad + 4(M_\pi^2-t)\Big((M_\pi^2-t)^2 + M_\pi^4 + t(s'+s''-u)\Big) \\ &\quad \times D_0(m_e^2,m_e^2,M_\pi^2,M_\pi^2,s,t,s',m_e^2,s'',M_\pi^2) \\ &\quad - 4(M_\pi^2-u)\Big((M_\pi^2-u)^2 + M_\pi^4 + u(s'+s''-t)\Big) \\ &\quad \times D_0(m_e^2,m_e^2,M_\pi^2,M_\pi^2,s,u,s',m_e^2,s'',M_\pi^2)\Big] + (\mathrm{Re}\to\mathrm{Im}),\end{aligned} \tag{3.2}$$

and loop functions C_0, D_0 in the conventions of ref. [77]. We stress that the presence of $|F_\pi^V(s)|^2$ in the denominator is just an effect of the normalization of the corrections δ to the

[1] One might wonder whether considering only the pion-pole contribution in the sub-amplitude $\gamma^*\gamma^* \to \pi\pi$ is a good approximation. To evaluate unitarity corrections to the pion-pole contribution one could start from a fixed-t instead of a fixed-s dispersion relation and make use of the full amplitudes for $\gamma^*\gamma^* \to \pi\pi$ [79–84]. However, as shown by these studies, below 1 GeV the Born terms yield the dominant contribution.

JHEP08(2022)295

Born cross section (1.2), whereas $F_\pi^V(s)$ in the numerator is due to the interference with the Born diagram.

3.1 Pole-pole

We first consider the case $s' = s'' = \lambda^2$. The IR divergences are easiest to extract using dispersive representations of the loop integrals, leading to the expressions given in appendix A.1. In combination, we find the following expression for the pole-pole contribution

$$\begin{aligned}
\delta_{\text{virt}}^{\text{pole-pole}} = \frac{\alpha}{\pi}\frac{\text{Re}\,F_\pi^V(s)}{|F_\pi^V(s)|^2}\Bigg\{&2\log\frac{\lambda^2}{s}\log\frac{1-\beta z}{1+\beta z} + \frac{z}{(1-z^2)\beta}\Bigg[\frac{(1-\beta)^2}{\beta}\frac{\pi^2}{6} + 2\log^2 2 \\
&- \log^2(1-\beta^2) + \frac{1+\beta^2}{2\beta}\left(4\text{Li}_2\left(\frac{\beta-1}{1+\beta}\right) + \log^2\frac{1-\beta}{1+\beta}\right)\Bigg] \\
&+ \frac{1+2\beta z+\beta^2}{(1-z^2)\beta^2}\left[\frac{1}{2}\log^2(1+\beta z) + \log\beta_+\log\frac{1+2\beta z+\beta^2}{1+\beta z} + \text{Li}_2(\beta_+)\right] \\
&- \frac{1-2\beta z+\beta^2}{(1-z^2)\beta^2}\left[\frac{1}{2}\log^2(1-\beta z) + \log\beta_-\log\frac{1-2\beta z+\beta^2}{1-\beta z} + \text{Li}_2(\beta_-)\right]\Bigg\} \\
+ \frac{\alpha}{\pi}\frac{\text{Im}\,F_\pi^V(s)}{|F_\pi^V(s)|^2}\frac{\pi}{(1-z^2)\beta^2}&\Bigg[(1+\beta^2)z\log\frac{1-\beta}{1+\beta} + 2\beta z\log\frac{1-\beta^2z^2}{1-\beta^2} \\
&- \Big(1+\beta^2(2z^2-1)\Big)\log\frac{1-\beta z}{1+\beta z}\Bigg], \qquad \beta_\pm = \frac{1-\beta^2}{2(1\pm\beta z)}.
\end{aligned} \tag{3.3}$$

The functional form of the contribution proportional to $\text{Re}\,F_\pi^V/|F_\pi^V|^2$ agrees with ref. [74], i.e., as expected, the point-like limit is recovered from the pole-pole contribution upon setting $F_\pi^V = 1$. In particular, we confirm that all collinear singularities cancel.

3.2 Pole-dispersive

The loop integrals required for the mixed pole and dispersive contributions are provided in appendix A.2. As a first step, we consider the IR divergence: for the real part, we find

$$\begin{aligned}
\delta_{\text{virt}}^{\text{pole-disp}}\big|_{\text{Re}}^{\text{IR}} &= \frac{\alpha}{\pi}\frac{\text{Re}\,F_\pi^V(s)}{|F_\pi^V(s)|^2}\left[2\log\frac{\lambda^2}{s}\log\frac{1-\beta z}{1+\beta z}\text{Re}\,\frac{s}{\pi}\int_{4M_\pi^2}^\infty ds'\frac{\text{Im}\,F_\pi^V(s')}{s'(s'-s)}\right] \\
&= \frac{\alpha}{\pi}\frac{\text{Re}\,F_\pi^V(s)}{|F_\pi^V(s)|^2}\left[2\log\frac{\lambda^2}{s}\log\frac{1-\beta z}{1+\beta z}(\text{Re}\,F_\pi^V(s)-1)\right],
\end{aligned} \tag{3.4}$$

which, together with eq. (3.3), combines to a prefactor $(\text{Re}\,F_\pi^V)^2/|F_\pi^V|^2$. The IR divergence in the imaginary part is more subtle. It arises from the imaginary part generated by the D_0 function for $s' < s$, since the integration over s' displays an end-point singularity at $s' = s$. To extract this singularity, we write

$$\begin{aligned}
\frac{1}{\pi}\int_{4M_\pi^2}^s ds'\frac{\text{Im}\,F_\pi^V(s')}{s'}\text{Im}\,\delta^{\text{pole-disp}}(s') &= \frac{1}{\pi}\int_{4M_\pi^2}^s ds'\frac{\text{Im}\,F_\pi^V(s')-\text{Im}\,F_\pi^V(s)}{s'}\text{Im}\,\delta^{\text{pole-disp}}(s') \\
&+ \frac{\text{Im}\,F_\pi^V(s)}{\pi}\int_{4M_\pi^2}^s ds'\frac{\text{Im}\,\delta^{\text{pole-disp}}(s')}{s'},
\end{aligned} \tag{3.5}$$

JHEP08(2022)295

with integrand

$$\begin{aligned}\operatorname{Im}\delta^{\text{pole-disp}}(s') = &\frac{2\pi\big(s'-s+(s+s'-2sz^2)\beta^2\big)\log\frac{1-\beta z}{1+\beta z}}{(s'-s)(1-z^2)\beta^2}\\ &-\frac{2\pi z\left((1+\beta^2)\log\frac{1-\beta}{1+\beta}+2\beta\log\frac{1-\beta^2z^2}{1-\beta^2}\right)}{(1-z^2)\beta^2}.\end{aligned}\tag{3.6}$$

The second integral in eq. (3.5), however, needs to be evaluated including the dominant effect of the IR regulator, which changes the imaginary part of the D_0 function to

$$\begin{aligned}\operatorname{Im} D_0(s,t,s',\lambda^2) = &\frac{2\pi\theta\left(\left(\sqrt{s}-\lambda\right)^2-s'\right)}{\sqrt{(s'-s)^2(M_\pi^2-t)^2-2\lambda^2\big((s+s')(M_\pi^2-t)^2+2ss't\big)}}\\ &\times\left(\log\frac{M_\pi^2-t}{s}+\log\frac{s}{m_eM_\pi}\right).\end{aligned}\tag{3.7}$$

The second term in the last line does not give rise to an IR divergence, and cancels with the other collinear singularities. For simplicity, we treat the regular terms in the same way as the singular ones, which slightly simplifies the expressions and allows us to write the full contribution from the imaginary part as

$$\begin{aligned}\delta_{\text{virt}}^{\text{pole-disp}}\big|_{\text{Im}} = &\frac{\alpha}{\pi}\frac{\operatorname{Im}F_\pi^V(s)}{|F_\pi^V(s)|^2}\left[\frac{1}{\pi}\int_{4M_\pi^2}^{s}ds'\frac{\operatorname{Im}F_\pi^V(s')-\operatorname{Im}F_\pi^V(s)}{s'}\operatorname{Im}\delta^{\text{pole-disp}}(s')\right]\\ &+\frac{\alpha}{\pi}\frac{\left(\operatorname{Im}F_\pi^V(s)\right)^2}{|F_\pi^V(s)|^2}\Bigg\{2\log\frac{4\lambda^2}{s}\log\frac{1-\beta z}{1+\beta z}\\ &\quad+4\log\frac{1-\beta z}{2}\log\left[1-\beta z+\sqrt{1-2\beta z+\beta^2}\right]-4\log^2(1-\beta z)\\ &\quad-4\log\frac{1+\beta z}{2}\log\left[1+\beta z+\sqrt{1+2\beta z+\beta^2}\right]+4\log^2(1+\beta z)\\ &\quad+\frac{2\log(1-\beta^2)}{(1-z^2)\beta^2}\left(z(1+\beta^2)\log\frac{1-\beta}{1+\beta}-\log\frac{1-\beta z}{1+\beta z}+2\beta z\log\frac{1-\beta^2z^2}{1-\beta^2}\right)\\ &\quad-\frac{2\log\frac{1-\beta z}{1+\beta z}}{1-z^2}\left((2z^2-1)\log\frac{1-\beta^2}{\beta^2}+2\log\beta\right)\Bigg\}.\end{aligned}\tag{3.8}$$

Summing up the IR divergences in eqs. (3.3), (3.4), and (3.8), we finally obtain

$$\delta_{\text{virt}}^{\text{IR}} = 2\frac{\alpha}{\pi}\log\frac{\lambda^2}{s}\log\frac{1-\beta z}{1+\beta z},\tag{3.9}$$

which cancels against the real emission (1.5), as expected. However, we stress that for the virtual contribution the factor $|F_\pi^V|^2$ originates from a subtle interplay of three different contributions, which no longer works for the finite terms: for the latter F_π^V remains buried inside dispersive integrals and neither factorizes nor combines into just the modulus squared. Ultimately, this is the reason why multiplying the point-like result by $|F_\pi^V|^2$ is a poor approximation.

JHEP08(2022)295

For completeness, we also give the full expression for the real part:

$$
\begin{aligned}
\delta_{\text{virt}}^{\text{pole-disp}}\big|_{\text{Re}} &= \frac{\alpha}{\pi}\frac{\text{Re}\,F_\pi^V(s)}{|F_\pi^V(s)|^2}\frac{1}{\pi}\int_{4M_\pi^2}^{\infty} ds' \frac{\text{Im}\,F_\pi^V(s')}{s'}\text{Re}\,\delta^{\text{pole-disp}}(s'),\\
\text{Re}\,\delta^{\text{pole-disp}} &= \frac{2s}{s'-s}\bigg[\log\frac{\lambda^2 s'}{(s'-s)^2}\log\frac{1-\beta z}{1+\beta z} + \text{Li}_2\bigg(1-\frac{s'(1-\beta')}{s(1-\beta z)}\bigg)\\
&\qquad + \text{Li}_2\bigg(1-\frac{s'(1+\beta')}{s(1-\beta z)}\bigg) - \text{Li}_2\bigg(1-\frac{s'(1-\beta')}{s(1+\beta z)}\bigg) - \text{Li}_2\bigg(1-\frac{s'(1+\beta')}{s(1+\beta z)}\bigg)\bigg]\\
&\quad + \frac{2(1+\beta^2)}{(1-z^2)\beta^2}\log\frac{1-\beta z}{1+\beta z}\log\frac{2s}{(1-\beta^2)|s-s'|}\\
&\quad - \frac{4z}{(1-z^2)\beta}\bigg[s\text{Re}\,\bar{C}_0(s,s',m_e^2) + \frac{s}{2}(1+\beta^2)\text{Re}\,C_0(s,s',M_\pi^2) + \log^2 2\\
&\qquad + \log^2(1-\beta') + \log^2(1+\beta') - \log^2(1-\beta^2) - \log\frac{1-\beta^2}{2}\log\left(1-\beta^2 z^2\right)\\
&\qquad + \log\frac{1-\beta^2 z^2}{(1-\beta^2)^2}\log\frac{s}{s'} - \log\frac{s'(1-\beta^2)}{s(1-\beta^2 z^2)}\log\frac{s'}{|s-s'|}\bigg]\\
&\quad + \frac{2(1-2\beta z+\beta^2)}{(1-z^2)\beta^2}\bigg[\text{Li}_2\bigg(1-\frac{s'(1-\beta')}{s(1-\beta z)}\bigg) + \text{Li}_2\bigg(1-\frac{s'(1+\beta')}{s(1-\beta z)}\bigg) + \text{Li}_2(\beta_-)\\
&\qquad + \log\left(1-2\beta z+\beta^2\right)\log\beta_- + \frac{3}{2}\log^2(1-\beta z)\bigg]\\
&\quad - \frac{2(1+2\beta z+\beta^2)}{(1-z^2)\beta^2}\bigg[\text{Li}_2\bigg(1-\frac{s'(1-\beta')}{s(1+\beta z)}\bigg) + \text{Li}_2\bigg(1-\frac{s'(1+\beta')}{s(1+\beta z)}\bigg) + \text{Li}_2(\beta_+)\\
&\qquad + \log\left(1+2\beta z+\beta^2\right)\log\beta_+ + \frac{3}{2}\log^2(1+\beta z)\bigg],
\end{aligned}
\tag{3.10}
$$

where

$$
\bar{C}_0(s,s',m_e^2) = \bigg[C_0(s,s',m_e^2) + \frac{\log\frac{m_e^2}{s'}\log\frac{|s'-s|}{s'}}{s}\bigg]_{m_e\to 0}
\tag{3.11}
$$

is the finite part of the massless $C_0(s,s',m_e^2)$ loop function and again all the collinear singularities from $m_e \to 0$ cancel. The singularity at $s'=s$ is to be interpreted as the principal value, but in contrast to the imaginary part no end-point singularity arises.

3.3 Dispersive-dispersive

The purely dispersive correction can be expressed as

$$
\begin{aligned}
\delta_{\text{virt}}^{\text{disp-disp}} &= \frac{\alpha}{\pi}\frac{\text{Re}\,F_\pi^V(s)}{|F_\pi^V(s)|^2}\frac{1}{\pi}\int_{4M_\pi^2}^{\infty} ds'\frac{\text{Im}\,F_\pi^V(s')}{s'}\frac{1}{\pi}\int_{4M_\pi^2}^{\infty} ds''\frac{\text{Im}\,F_\pi^V(s'')}{s''}\text{Re}\,\delta^{\text{disp-disp}}(s',s'')\\
&\quad + \frac{\alpha}{\pi}\frac{\text{Im}\,F_\pi^V(s)}{|F_\pi^V(s)|^2}\frac{1}{\pi}\int_{4M_\pi^2}^{\infty} ds'\frac{\text{Im}\,F_\pi^V(s')}{s'}\frac{1}{\pi}\int_{4M_\pi^2}^{\infty} ds''\frac{\text{Im}\,F_\pi^V(s'')}{s''}\text{Im}\,\delta^{\text{disp-disp}}(s',s''),
\end{aligned}
\tag{3.12}
$$

where the integrands follow directly from eq. (3.2). All loop functions that contribute in this case, explicit expressions for which are provided in appendix A.3, are IR finite and free of collinear singularities.

JHEP08(2022)295

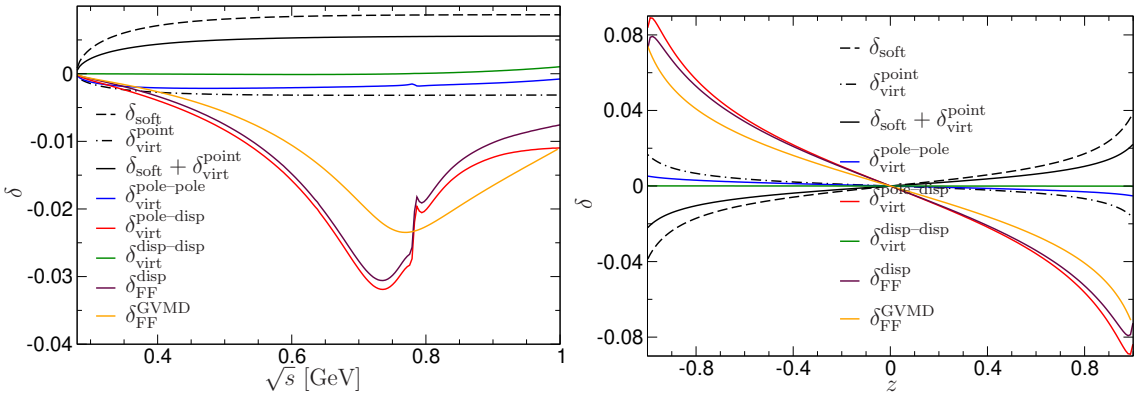

Figure 2. Correction factors δ as a function of $\sqrt{s}$ for fixed $z = \cos(1)$ (left) and as a function of z for fixed $\sqrt{s} = 0.75\,\text{GeV}$ (right). The black lines denote the point-like result (dashed: real, dot-dashed: virtual, solid: sum of real and virtual), where in all cases the logarithmic terms including the IR divergence are not shown. In the same convention, we show our results for the pole-pole (blue), pole-dispersive (red), and dispersive-dispersive (green) contributions, as well as their sum minus the point-like virtual correction (maroon). The same quantity in the GVMD model of ref. [75] with a single Breit-Wigner is given for comparison (orange).

4 Numerical analysis

For the numerical analysis we use the pion VFF from ref. [4] for $s \leq s_{\text{cut}}$, $s_{\text{cut}} = 1\,\text{GeV}^2$. Since the corrections δ are defined relative to the tree-level result (1.2), which itself depends on F_π^V, they need to be determined in a self-consistent way. Accordingly, we restrict the analysis here to the energy below s_{cut}. However, for the dispersive integrals we also need to provide $\text{Im}\,F_\pi^V$ above, in particular, in writing eq. (2.4) we have implicitly assumed the sum rule

$$\frac{1}{\pi}\int_{4M_\pi^2}^{\infty} ds' \frac{\text{Im}\,F_\pi^V(s')}{s'} = 1. \tag{4.1}$$

In practice, this sum rule is easiest to fulfill by including excited ρ', ρ'' resonances in the $\pi\pi$ phase shift, which is one of the variants for the asymptotic continuation studied in ref. [4] (using the implementation from ref. [85], based on the data from ref. [86]). In the following, we use the corresponding input for F_π^V.

Our numerical results for the corrections δ are shown in figures 2 and 3, where in all cases the terms proportional to $\log\frac{\lambda^2}{4\Delta^2}$ and $\log\frac{\lambda^2}{s}$, respectively, are dropped. In addition to the separate curves for the pole-pole, pole-dispersive, and dispersive-dispersive contributions, we also show the quantity δ_{FF}, which was defined in ref. [75] as the total minus the point-like virtual correction. We also include the GVMD model from the same reference (in the variant using a single Breit-Wigner function for the $\rho(770)$), and, in figure 2, choose the same fixed parameters ($z = \cos(1)$ and $\sqrt{s} = 0.75\,\text{GeV}$, respectively) to facilitate the comparison. Figure 3 shows our results for δ_{FF} as a function of both $\sqrt{s}$ and z.

The main observation is that we confirm significant departures from the point-like approximation, which, as remarked in the previous section, are a remnant of the intricate manner how IR singularities cancel in the sum of real and virtual contributions for a general

JHEP08(2022)295

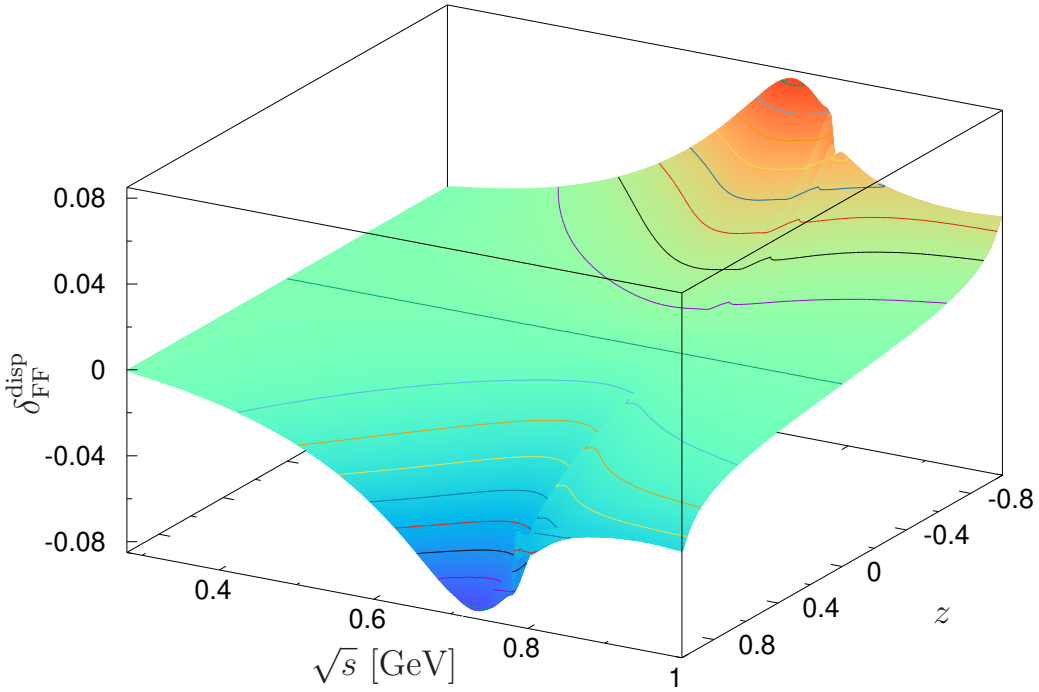

Figure 3. Structure-dependent correction $\delta_{\rm FF}$ in the dispersive approach (sum of pole-pole, pole-dispersive, and dispersive-dispersive minus point-like virtual), as a function of $\sqrt{s}$ and z. The contour lines give increments of 0.01. A data file is attached as supplemental material.

VFF. In particular, while the pole-pole piece remains small and actually stays close to the point-like result, the pole-dispersive correction receives a large enhancement in the vicinity of the ρ resonance. The exact shape does differ when compared to the GVMD approximation, but the overall size of the effect seems to be captured correctly by the model. Finally, we find that the dispersive-dispersive contributions are negligible below 1 GeV, supporting the expectation that the most important radiative corrections are the ones that display some form of IR enhancement.

5 Conclusions

In this paper we presented a calculation of the radiative corrections to the forward-backward asymmetry in $e^+e^- \to \pi^+\pi^-$ that includes the full effect of the pion vector form factor in the loop integral by means of a dispersive representation and thus captures the leading hadronic intermediate state. In particular, we studied how the cancellation of infrared divergences proceeds in the case of a general form factor, and found that an intricate interplay between a point-like pion-pole contribution and the real and imaginary parts of a mixed pole and dispersive correction becomes necessary. Overall, the numerical results support recent findings in a generalized vector-meson-dominance model [75], indicating significant deviations from the point-like approximation, but the dispersive analysis puts this conclusion on a more solid foundation and allows one to trace back the origin of the large correction to a remnant of the infrared singularities. This implies that the usual

JHEP08(2022)295

assumption that the most important radiative corrections for processes involving hadrons should be the ones that display some form of infrared enhancement actually proves correct, while the problem in the scalar-QED calculation multiplied by the pion vector form factor was that these pieces were not correctly identified. These insights should prove valuable for reassessing the role of radiative corrections in precision measurements of $e^+e^- \to \pi^+\pi^-$.

Acknowledgments

We thank Peter Stoffer for comments on the manuscript. Financial support by the SNSF (Project Nos. 200020_175791, PCEFP2_181117, and PZ00P2_174228) and by the Ramón y Cajal program (RYC2019-027605-I) of the Spanish MINECO is gratefully acknowledged.

A Loop functions

A.1 Pole-pole

For the pole-pole contribution we need the loop functions for $s' = s'' = \lambda^2$:

$$
\begin{aligned}
C_0(t,\lambda^2) &= \frac{1}{M_\pi^2 - t}\bigg[\log\frac{\lambda^2}{M_\pi^2}\log\frac{M_\pi^2 - t}{M_\pi m_e} + \log^2\frac{m_e}{M_\pi} - \log^2\frac{M_\pi^2 - t}{M_\pi^2} - \mathrm{Li}_2\bigg(\frac{t}{M_\pi^2}\bigg)\bigg],\\
C_0(s,\lambda^2,\lambda^2,M_\pi^2) &= \frac{1}{s\beta}\bigg[\frac{\pi^2}{6} + \frac{1}{2}\log^2\frac{1-\beta}{1+\beta} + 2\mathrm{Li}_2\bigg(\frac{\beta-1}{1+\beta}\bigg) + i\pi\log\frac{1-\beta}{1+\beta}\bigg],\\
C_0(s,\lambda^2,\lambda^2,m_e^2) &= \frac{\pi^2 + 3\log^2\frac{m_e^2}{s} + 6i\pi\log\frac{m_e^2}{s}}{6s},\\
D_0(s,t,\lambda^2,\lambda^2) &= \frac{2}{s}\bigg(\log\frac{\lambda^2}{s} + i\pi\bigg)\frac{\log\frac{M_\pi^2 - t}{m_e M_\pi}}{M_\pi^2 - t},
\end{aligned}
\tag{A.1}
$$

where we suppressed the other arguments and only kept m_e to regularize collinear singularities at intermediate steps of the calculation.

A.2 Pole-dispersive

For the case $s' \geq 4M_\pi^2$, $s'' = \lambda^2$ we need the additional loop functions

$$
\begin{aligned}
C_0(t,s') = -\frac{1}{M_\pi^2 - t}\bigg[&\mathrm{Li}_2\bigg(\frac{t}{M_\pi^2}\bigg) + \mathrm{Li}_2\bigg(1 - \frac{s'(1-\beta')}{2(M_\pi^2 - t)}\bigg) + \mathrm{Li}_2\bigg(1 - \frac{s'(1+\beta')}{2(M_\pi^2 - t)}\bigg)\\
&+ \frac{\pi^2}{6} + \frac{1}{2}\log^2(1-\beta') + \frac{1}{2}\log^2(1+\beta') - \log\frac{2M_\pi^2}{M_\pi^2 - t}\log\frac{2(M_\pi^2 - t)}{s'}\bigg],\\
C_0^{>}(s,s',M_\pi^2) = \frac{1}{s\beta}\bigg[&\mathrm{Li}_2\bigg(\frac{1-\beta}{1-\beta'}\bigg) + \mathrm{Li}_2\bigg(\frac{1+\beta'}{1+\beta}\bigg) + \mathrm{Li}_2\bigg(\frac{1-\beta}{1+\beta'}\bigg) + \mathrm{Li}_2\bigg(\frac{1-\beta'}{1+\beta}\bigg)\\
&+ \frac{1}{2}\bigg(\log^2\frac{1-\beta}{1+\beta} + \log^2\frac{1+\beta}{1+\beta'} + \log^2\frac{1+\beta}{1-\beta'} + 2\log\frac{1+\beta'}{1-\beta'}\log\frac{\beta-\beta'}{\beta+\beta'}\bigg)\\
&- \frac{\pi^2}{2} + 2\mathrm{Li}_2\bigg(\frac{\beta-1}{1+\beta}\bigg) + i\pi\log\frac{1-\beta}{1+\beta}\bigg],\\
C_0^{>}(s,s',m_e^2) = &\frac{-\frac{\pi^2}{3} + \frac{1}{2}\log^2\frac{s}{s'} - \log\frac{m_e^2}{s'}\log\frac{s-s'}{s'} + \mathrm{Li}_2\left(\frac{s'}{s}\right) + i\pi\log\frac{m_e^2}{s}}{s},
\end{aligned}
$$

$$
\begin{aligned}
C_0^<(s,s',M_\pi^2) &= \frac{1}{s\beta}\bigg[-\mathrm{Li}_2\Big(\frac{1-\beta'}{1-\beta}\Big)-\mathrm{Li}_2\Big(\frac{1+\beta}{1+\beta'}\Big)+\mathrm{Li}_2\Big(\frac{1-\beta}{1+\beta'}\Big)+\mathrm{Li}_2\Big(\frac{1-\beta'}{1+\beta}\Big)\\
&\quad+\frac{1}{2}\Big(\log^2\frac{1-\beta}{1+\beta}-\log^2\frac{1-\beta}{1-\beta'}+\log^2\frac{1+\beta}{1-\beta'}+2\log\frac{1+\beta'}{1-\beta'}\log\frac{\beta'-\beta}{\beta+\beta'}\Big)\\
&\quad+\frac{\pi^2}{6}+2\mathrm{Li}_2\Big(\frac{\beta-1}{1+\beta}\Big)\bigg],\\
C_0^<(s,s',m_e^2) &= \frac{-\log\frac{m_e^2}{s'}\log\frac{s'-s}{s'}-\mathrm{Li}_2\left(\frac{s}{s'}\right)}{s},\\
D_0(s,t,s',\lambda^2) &= -\frac{\log\frac{M_\pi^2-t}{m_eM_\pi}\left[\log\frac{\lambda^2}{M_\pi^2}-\log\frac{m_e}{M_\pi}+\log\frac{s'^2}{(s'-s)^2}-\log\frac{M_\pi^2-t}{M_\pi^2}+2\pi i\theta(s-s')\right]}{(M_\pi^2-t)(s'-s)}\\
&\quad-\frac{1}{(M_\pi^2-t)(s'-s)}\bigg[\frac{\pi^2}{6}+\mathrm{Li}_2\Big(1-\frac{s'(1-\beta')}{2(M_\pi^2-t)}\Big)+\mathrm{Li}_2\Big(1-\frac{s'(1+\beta')}{2(M_\pi^2-t)}\Big)\\
&\quad+\frac{1}{2}\log^2(1-\beta')+\frac{1}{2}\log^2(1+\beta')-\log\frac{2M_\pi^2}{M_\pi^2-t}\log\frac{2(M_\pi^2-t)}{s'}\bigg],
\end{aligned}
\tag{A.2}
$$

where $\beta'=\sqrt{1-4M_\pi^2/s'}$ and $\gtrless$ indicates that the expression applies to $s\gtrless s'$.

A.3 Dispersive-dispersive

For general s',s'' we write the additional loop functions in the form

$$
C_0(s,s',s'',M_\pi^2)=\frac{1}{\pi}\int_{\left(\sqrt{s'}+\sqrt{s''}\right)^2}^{\infty}dx\frac{\mathrm{Im}\,C_0(x,s',s'',M_\pi^2)}{x-s},
\tag{A.3}
$$

$$
\begin{aligned}
\mathrm{Im}\,C_0(s,s',s'',M_\pi^2) &= \frac{\pi\theta\left(s-\left(\sqrt{s'}+\sqrt{s''}\right)^2\right)}{s\beta}\log\frac{s-s'-s''-\beta\lambda_s^{1/2}}{s-s'-s''+\beta\lambda_s^{1/2}},\\
D_0(s,t,s',s'') &= \frac{1}{\pi}\int_{M_\pi^2}^{\infty}dx\frac{\mathrm{Im}_t\,D_0(s,x,s',s'')}{x-t}=\frac{1}{\pi}\int_{\left(\sqrt{s'}+\sqrt{s''}\right)^2}^{\infty}dx\frac{\mathrm{Im}_s\,D_0(x,t,s',s'')}{x-s},\\
\mathrm{Im}_t\,D_0^>(s,t,s',s'') &= \frac{\pi\theta(t-M_\pi^2)}{\sqrt{\Delta(s,t,s',s'')}}\bigg[2\pi i\theta\left(s-\left(\sqrt{s'}+\sqrt{s''}\right)^2\right)\\
&\quad+\log\frac{(s'+s''-s)(M_\pi^2-t)^2+2ts's''+(t-M_\pi^2)\sqrt{\Delta(s,t,s',s'')}}{(s'+s''-s)(M_\pi^2-t)^2+2ts's''-(t-M_\pi^2)\sqrt{\Delta(s,t,s',s'')}}\bigg],\\
\mathrm{Im}_t\,D_0^<(s,t,s',s'') &= \frac{2\pi\theta(t-M_\pi^2)}{\sqrt{-\Delta(s,t,s',s'')}}\bigg[\arctan\frac{(t-M_\pi^2)\sqrt{-\Delta(s,t,s',s'')}}{(s'+s''-s)(M_\pi^2-t)^2+2ts's''}\\
&\quad+\pi\theta\Big((s-s'-s'')(M_\pi^2-t)^2-2ts's''\Big)\bigg],\\
\mathrm{Im}_s\,D_0(s,t,s',s'') &= \frac{\pi\theta\left(s-\left(\sqrt{s'}+\sqrt{s''}\right)^2\right)}{\sqrt{\Delta(s,t,s',s'')}}\log\frac{2ss's''+\lambda_s(M_\pi^2-t)+\sqrt{\lambda_s\Delta(s,t,s',s'')}}{2ss's''+\lambda_s(M_\pi^2-t)-\sqrt{\lambda_s\Delta(s,t,s',s'')}},
\end{aligned}
$$

where

$$
\Delta(s,t,s',s'')=\lambda_s(M_\pi^2-t)^2-4tss's'',\qquad \lambda_s=\lambda(s,s',s''),
\tag{A.4}
$$

$\lambda(a,b,c)=a^2+b^2+c^2-2(ab+ac+bc)$, and the expressions are valid in the kinematic region of interest ($s'\geq 4M_\pi^2$, $s''\geq 4M_\pi^2$, $s\geq 4M_\pi^2$, $t\leq 0$, $m_e=0$). $\gtrless$ indicates that the expression applies for $\Delta(s,t,s',s'')\gtrless 0$.

JHEP08(2022)295

References

[1] T. Aoyama et al., *The anomalous magnetic moment of the muon in the Standard Model*, *Phys. Rept.* **887** (2020) 1 [arXiv:2006.04822] [INSPIRE].

[2] M. Davier, A. Hoecker, B. Malaescu and Z. Zhang, *Reevaluation of the hadronic vacuum polarisation contributions to the Standard Model predictions of the muon $g-2$ and $\alpha(m_Z^2)$ using newest hadronic cross-section data*, *Eur. Phys. J. C* **77** (2017) 827 [arXiv:1706.09436] [INSPIRE].

[3] A. Keshavarzi, D. Nomura and T. Teubner, *Muon $g-2$ and $\alpha(M_Z^2)$: a new data-based analysis*, *Phys. Rev. D* **97** (2018) 114025 [arXiv:1802.02995] [INSPIRE].

[4] G. Colangelo, M. Hoferichter and P. Stoffer, *Two-pion contribution to hadronic vacuum polarization*, *JHEP* **02** (2019) 006 [arXiv:1810.00007] [INSPIRE].

[5] M. Hoferichter, B.-L. Hoid and B. Kubis, *Three-pion contribution to hadronic vacuum polarization*, *JHEP* **08** (2019) 137 [arXiv:1907.01556] [INSPIRE].

[6] M. Davier, A. Hoecker, B. Malaescu and Z. Zhang, *A new evaluation of the hadronic vacuum polarisation contributions to the muon anomalous magnetic moment and to $\alpha(m_Z^2)$*, *Eur. Phys. J. C* **80** (2020) 241 [*Erratum ibid.* **80** (2020) 410] [arXiv:1908.00921] [INSPIRE].

[7] A. Keshavarzi, D. Nomura and T. Teubner, *$g-2$ of charged leptons, $\alpha(M_Z^2)$, and the hyperfine splitting of muonium*, *Phys. Rev. D* **101** (2020) 014029 [arXiv:1911.00367] [INSPIRE].

[8] M.N. Achasov et al., *Study of the process $e^+e^- \to \pi^+\pi^-$ in the energy region $400 < \sqrt{s} < 1000$ MeV*, *J. Exp. Theor. Phys.* **101** (2005) 1053 [hep-ex/0506076] [INSPIRE].

[9] M.N. Achasov et al., *Update of the $e^+e^- \to \pi^+\pi^-$ cross-section measured by SND detector in the energy region $400 < \sqrt{s} < 1000$ MeV*, *J. Exp. Theor. Phys.* **103** (2006) 380 [hep-ex/0605013] [INSPIRE].

[10] CMD-2 collaboration, *Measurement of $e^+e^- \to \pi^+\pi^-$ cross-section with CMD-2 around ρ meson*, *Phys. Lett. B* **527** (2002) 161 [hep-ex/0112031] [INSPIRE].

[11] CMD-2 collaboration, *Reanalysis of hadronic cross-section measurements at CMD-2*, *Phys. Lett. B* **578** (2004) 285 [hep-ex/0308008] [INSPIRE].

[12] V.M. Aul'chenko et al., *Measurement of the $e^+e^- \to \pi^+\pi^-$ cross section with the CMD-2 detector in the 370–520-MeV c.m. energy range*, *JETP Lett.* **84** (2006) 413 [hep-ex/0610016] [INSPIRE].

[13] CMD-2 collaboration, *High-statistics measurement of the pion form factor in the ρ-meson energy range with the CMD-2 detector*, *Phys. Lett. B* **648** (2007) 28 [hep-ex/0610021] [INSPIRE].

[14] BESIII collaboration, *Measurement of the $e^+e^- \to \pi^+\pi^-$ cross section between 600 and 900 MeV using initial state radiation*, *Phys. Lett. B* **753** (2016) 629 [*Erratum ibid.* **812** (2021) 135982] [arXiv:1507.08188] [INSPIRE].

JHEP08(2022)295

[15] T. Xiao, S. Dobbs, A. Tomaradze, K.K. Seth and G. Bonvicini, *Precision Measurement of the Hadronic Contribution to the Muon Anomalous Magnetic Moment*, *Phys. Rev. D* **97** (2018) 032012 [arXiv:1712.04530] [INSPIRE].

[16] B. Ananthanarayan, I. Caprini and D. Das, *Pion electromagnetic form factor at high precision with implications to $a_\mu^{\pi\pi}$ and the onset of perturbative QCD*, *Phys. Rev. D* **98** (2018) 114015 [arXiv:1810.09265] [INSPIRE].

[17] D. Stamen, D. Hariharan, M. Hoferichter, B. Kubis and P. Stoffer, *Kaon electromagnetic form factors in dispersion theory*, *Eur. Phys. J. C* **82** (2022) 432 [arXiv:2202.11106] [INSPIRE].

[18] E.B. Dally et al., *Elastic Scattering Measurement of the Negative Pion Radius*, *Phys. Rev. Lett.* **48** (1982) 375 [INSPIRE].

[19] NA7 collaboration, *A Measurement of the Space-Like Pion Electromagnetic Form-Factor*, *Nucl. Phys. B* **277** (1986) 168 [INSPIRE].

[20] BaBar collaboration, *Precise measurement of the $e^+e^- \to \pi^+\pi^-(\gamma)$ cross section with the Initial State Radiation method at BABAR*, *Phys. Rev. Lett.* **103** (2009) 231801 [arXiv:0908.3589] [INSPIRE].

[21] BaBar collaboration, *Precise Measurement of the $e^+e^- \to \pi^+\pi^-(\gamma)$ Cross Section with the Initial-State Radiation Method at BABAR*, *Phys. Rev. D* **86** (2012) 032013 [arXiv:1205.2228] [INSPIRE].

[22] KLOE collaboration, *Measurement of $\sigma(e^+e^- \to \pi^+\pi^-\gamma(\gamma))$ and the dipion contribution to the muon anomaly with the KLOE detector*, *Phys. Lett. B* **670** (2009) 285 [arXiv:0809.3950] [INSPIRE].

[23] KLOE collaboration, *Measurement of $\sigma(e^+e^- \to \pi^+\pi^-)$ from threshold to 0.85 GeV^2 using Initial State Radiation with the KLOE detector*, *Phys. Lett. B* **700** (2011) 102 [arXiv:1006.5313] [INSPIRE].

[24] KLOE collaboration, *Precision measurement of $\sigma(e^+e^- \to \pi^+\pi^-\gamma)/\sigma(e^+e^- \to \mu^+\mu^-\gamma)$ and determination of the $\pi^+\pi^-$ contribution to the muon anomaly with the KLOE detector*, *Phys. Lett. B* **720** (2013) 336 [arXiv:1212.4524] [INSPIRE].

[25] KLOE-2 collaboration, *Combination of KLOE $\sigma\left(e^+e^- \to \pi^+\pi^-\gamma(\gamma)\right)$ measurements and determination of $a_\mu^{\pi^+\pi^-}$ in the energy range $0.10 < s < 0.95$ GeV^2*, *JHEP* **03** (2018) 173 [arXiv:1711.03085] [INSPIRE].

[26] SND collaboration, *Measurement of the $e^+e^- \to \pi^+\pi^-$ process cross section with the SND detector at the VEPP-2000 collider in the energy region $0.525 < \sqrt{s} < 0.883$ GeV*, *JHEP* **01** (2021) 113 [arXiv:2004.00263] [INSPIRE].

[27] A.E. Ryzhenenkov et al., *Overview of the CMD-3 recent results*, *J. Phys. Conf. Ser.* **1526** (2020) 012009 [INSPIRE].

[28] G. Abbiendi et al., *Mini-Proceedings of the STRONG2020 Virtual Workshop on "Space-like and Time-like determination of the Hadronic Leading Order contribution to the Muon $g-2$"*, arXiv:2201.12102 [INSPIRE].

[29] BESIII collaboration, *Future Physics Programme of BESIII*, *Chin. Phys. C* **44** (2020) 040001 [arXiv:1912.05983] [INSPIRE].

[30] Belle-II collaboration, *The Belle II Physics Book*, *PTEP* **2019** (2019) 123C01 [*Erratum ibid.* **2020** (2020) 029201] [arXiv:1808.10567] [INSPIRE].

JHEP08(2022)295

[31] S. Borsányi et al., *Leading hadronic contribution to the muon magnetic moment from lattice QCD*, *Nature* **593** (2021) 51 [arXiv:2002.12347] [INSPIRE].

[32] M. Cè et al., *Window observable for the hadronic vacuum polarization contribution to the muon $g-2$ from lattice QCD*, arXiv:2206.06582 [INSPIRE].

[33] C. Alexandrou et al., *Lattice calculation of the short and intermediate time-distance hadronic vacuum polarization contributions to the muon magnetic moment using twisted-mass fermions*, arXiv:2206.15084 [INSPIRE].

[34] RBC and UKQCD collaborations, *Calculation of the hadronic vacuum polarization contribution to the muon anomalous magnetic moment*, *Phys. Rev. Lett.* **121** (2018) 022003 [arXiv:1801.07224] [INSPIRE].

[35] A. Crivellin, M. Hoferichter, C.A. Manzari and M. Montull, *Hadronic Vacuum Polarization: $(g-2)_\mu$ versus Global Electroweak Fits*, *Phys. Rev. Lett.* **125** (2020) 091801 [arXiv:2003.04886] [INSPIRE].

[36] A. Keshavarzi, W.J. Marciano, M. Passera and A. Sirlin, *Muon $g-2$ and $\Delta\alpha$ connection*, *Phys. Rev. D* **102** (2020) 033002 [arXiv:2006.12666] [INSPIRE].

[37] B. Malaescu and M. Schott, *Impact of correlations between a_μ and α_{QED} on the EW fit*, *Eur. Phys. J. C* **81** (2021) 46 [arXiv:2008.08107] [INSPIRE].

[38] G. Colangelo, M. Hoferichter and P. Stoffer, *Constraints on the two-pion contribution to hadronic vacuum polarization*, *Phys. Lett. B* **814** (2021) 136073 [arXiv:2010.07943] [INSPIRE].

[39] G. Colangelo et al., *Data-driven evaluations of Euclidean windows to scrutinize hadronic vacuum polarization*, *Phys. Lett. B* **833** (2022) 137313 [arXiv:2205.12963] [INSPIRE].

[40] Muon g-2 collaboration, *Final Report of the Muon E821 Anomalous Magnetic Moment Measurement at BNL*, *Phys. Rev. D* **73** (2006) 072003 [hep-ex/0602035] [INSPIRE].

[41] Muon g-2 collaboration, *Measurement of the Positive Muon Anomalous Magnetic Moment to 0.46 ppm*, *Phys. Rev. Lett.* **126** (2021) 141801 [arXiv:2104.03281] [INSPIRE].

[42] Muon g-2 collaboration, *Magnetic-field measurement and analysis for the Muon $g-2$ Experiment at Fermilab*, *Phys. Rev. A* **103** (2021) 042208 [arXiv:2104.03201] [INSPIRE].

[43] Muon g-2 collaboration, *Beam dynamics corrections to the Run-1 measurement of the muon anomalous magnetic moment at Fermilab*, *Phys. Rev. Accel. Beams* **24** (2021) 044002 [arXiv:2104.03240] [INSPIRE].

[44] Muon g-2 collaboration, *Measurement of the anomalous precession frequency of the muon in the Fermilab Muon $g-2$ Experiment*, *Phys. Rev. D* **103** (2021) 072002 [arXiv:2104.03247] [INSPIRE].

[45] T. Aoyama, M. Hayakawa, T. Kinoshita and M. Nio, *Complete Tenth-Order QED Contribution to the Muon g-2*, *Phys. Rev. Lett.* **109** (2012) 111808 [arXiv:1205.5370] [INSPIRE].

[46] T. Aoyama, T. Kinoshita and M. Nio, *Theory of the Anomalous Magnetic Moment of the Electron*, *Atoms* **7** (2019) 28 [INSPIRE].

[47] A. Czarnecki, W.J. Marciano and A. Vainshtein, *Refinements in electroweak contributions to the muon anomalous magnetic moment*, *Phys. Rev. D* **67** (2003) 073006 [*Erratum ibid.* **73** (2006) 119901] [hep-ph/0212229] [INSPIRE].

JHEP08(2022)295

[48] C. Gnendiger, D. Stöckinger and H. Stöckinger-Kim, *The electroweak contributions to* $(g-2)_\mu$ *after the Higgs boson mass measurement*, *Phys. Rev. D* **88** (2013) 053005 [arXiv:1306.5546] [INSPIRE].

[49] B.-L. Hoid, M. Hoferichter and B. Kubis, *Hadronic vacuum polarization and vector-meson resonance parameters from* $e^+e^- \to \pi^0\gamma$, *Eur. Phys. J. C* **80** (2020) 988 [arXiv:2007.12696] [INSPIRE].

[50] A. Kurz, T. Liu, P. Marquard and M. Steinhauser, *Hadronic contribution to the muon anomalous magnetic moment to next-to-next-to-leading order*, *Phys. Lett. B* **734** (2014) 144 [arXiv:1403.6400] [INSPIRE].

[51] K. Melnikov and A. Vainshtein, *Hadronic light-by-light scattering contribution to the muon anomalous magnetic moment revisited*, *Phys. Rev. D* **70** (2004) 113006 [hep-ph/0312226] [INSPIRE].

[52] P. Masjuan and P. Sánchez-Puertas, *Pseudoscalar-pole contribution to the* $(g_\mu - 2)$*: a rational approach*, *Phys. Rev. D* **95** (2017) 054026 [arXiv:1701.05829] [INSPIRE].

[53] G. Colangelo, M. Hoferichter, M. Procura and P. Stoffer, *Rescattering effects in the hadronic-light-by-light contribution to the anomalous magnetic moment of the muon*, *Phys. Rev. Lett.* **118** (2017) 232001 [arXiv:1701.06554] [INSPIRE].

[54] G. Colangelo, M. Hoferichter, M. Procura and P. Stoffer, *Dispersion relation for hadronic light-by-light scattering: two-pion contributions*, *JHEP* **04** (2017) 161 [arXiv:1702.07347] [INSPIRE].

[55] M. Hoferichter, B.-L. Hoid, B. Kubis, S. Leupold and S.P. Schneider, *Pion-pole contribution to hadronic light-by-light scattering in the anomalous magnetic moment of the muon*, *Phys. Rev. Lett.* **121** (2018) 112002 [arXiv:1805.01471] [INSPIRE].

[56] M. Hoferichter, B.-L. Hoid, B. Kubis, S. Leupold and S.P. Schneider, *Dispersion relation for hadronic light-by-light scattering: pion pole*, *JHEP* **10** (2018) 141 [arXiv:1808.04823] [INSPIRE].

[57] A. Gérardin, H.B. Meyer and A. Nyffeler, *Lattice calculation of the pion transition form factor with* $N_f = 2+1$ *Wilson quarks*, *Phys. Rev. D* **100** (2019) 034520 [arXiv:1903.09471] [INSPIRE].

[58] J. Bijnens, N. Hermansson-Truedsson and A. Rodríguez-Sánchez, *Short-distance constraints for the HLbL contribution to the muon anomalous magnetic moment*, *Phys. Lett. B* **798** (2019) 134994 [arXiv:1908.03331] [INSPIRE].

[59] G. Colangelo, F. Hagelstein, M. Hoferichter, L. Laub and P. Stoffer, *Short-distance constraints on hadronic light-by-light scattering in the anomalous magnetic moment of the muon*, *Phys. Rev. D* **101** (2020) 051501 [arXiv:1910.11881] [INSPIRE].

[60] G. Colangelo, F. Hagelstein, M. Hoferichter, L. Laub and P. Stoffer, *Longitudinal short-distance constraints for the hadronic light-by-light contribution to* $(g-2)_\mu$ *with large-*N_c *Regge models*, *JHEP* **03** (2020) 101 [arXiv:1910.13432] [INSPIRE].

[61] T. Blum et al., *Hadronic Light-by-Light Scattering Contribution to the Muon Anomalous Magnetic Moment from Lattice QCD*, *Phys. Rev. Lett.* **124** (2020) 132002 [arXiv:1911.08123] [INSPIRE].

[62] G. Colangelo, M. Hoferichter, A. Nyffeler, M. Passera and P. Stoffer, *Remarks on higher-order hadronic corrections to the muon* $g-2$, *Phys. Lett. B* **735** (2014) 90 [arXiv:1403.7512] [INSPIRE].

JHEP08(2022)295

[63] Working Group on Radiative Corrections, Monte Carlo Generators for Low Energies collaboration, *Quest for precision in hadronic cross sections at low energy: Monte Carlo tools vs. experimental data*, *Eur. Phys. J. C* **66** (2010) 585 [arXiv:0912.0749] [INSPIRE].

[64] G. Colangelo et al., *Prospects for precise predictions of a_μ in the Standard Model*, arXiv:2203.15810 [INSPIRE].

[65] F. Campanario et al., *Standard model radiative corrections in the pion form factor measurements do not explain the a_μ anomaly*, *Phys. Rev. D* **100** (2019) 076004 [arXiv:1903.10197] [INSPIRE].

[66] A. Hoefer, J. Gluza and F. Jegerlehner, *Pion pair production with higher order radiative corrections in low energy e^+e^- collisions*, *Eur. Phys. J. C* **24** (2002) 51 [hep-ph/0107154] [INSPIRE].

[67] H. Czyż, A. Grzelińska, J.H. Kühn and G. Rodrigo, *The radiative return at ϕ- and B-factories: FSR for muon pair production at next-to-leading order*, *Eur. Phys. J. C* **39** (2005) 411 [hep-ph/0404078] [INSPIRE].

[68] J. Gluza, A. Hoefer, S. Jadach and F. Jegerlehner, *Measuring the FSR inclusive $\pi^+\pi^-$ cross-section*, *Eur. Phys. J. C* **28** (2003) 261 [hep-ph/0212386] [INSPIRE].

[69] Y.M. Bystritskiy, E.A. Kuraev, G.V. Fedotovich and F.V. Ignatov, *The cross sections of the muons and charged pions pairs production at electron-positron annihilation near the threshold*, *Phys. Rev. D* **72** (2005) 114019 [hep-ph/0505236] [INSPIRE].

[70] J. Monnard, *Radiative corrections for the two-pion contribution to the hadronic vacuum polarization contribution to the muon $g-2$*, Ph.D. Thesis, Bern University, Switzerland (2020), https://boristheses.unibe.ch/2825/.

[71] S. Binner, J.H. Kühn and K. Melnikov, *Measuring $\sigma(e^+e^- \to hadrons)$ using tagged photon*, *Phys. Lett. B* **459** (1999) 279 [hep-ph/9902399] [INSPIRE].

[72] H. Czyż, A. Grzelińska and J.H. Kühn, *Charge asymmetry and radiative ϕ decays*, *Phys. Lett. B* **611** (2005) 116 [hep-ph/0412239] [INSPIRE].

[73] BaBar collaboration, *Measurement of initial-state-final-state radiation interference in the processes $e^+e^- \to \mu^+\mu^-\gamma$ and $e^+e^- \to \pi^+\pi^-\gamma$*, *Phys. Rev. D* **92** (2015) 072015 [arXiv:1508.04008] [INSPIRE].

[74] A.B. Arbuzov, T.V. Kopylova and G.A. Seilkhanova, *Forward-backward asymmetry in electron-positron annihilation into pion or kaon pairs revisited*, *Mod. Phys. Lett. A* **35** (2020) 2050210 [arXiv:2003.14054] [INSPIRE].

[75] F. Ignatov and R.N. Lee, *Charge asymmetry in $e^+e^- \to \pi^+\pi^-$ process*, *Phys. Lett. B* **833** (2022) 137283 [arXiv:2204.12235] [INSPIRE].

[76] S.H. Patil and S.D. Rindani, *Enhancement of Asymmetry in Lepton Annihilation Due to Resonances*, *Phys. Rev. D* **13** (1976) 730 [INSPIRE].

[77] A. Denner, *Techniques for calculation of electroweak radiative corrections at the one loop level and results for W physics at LEP-200*, *Fortsch. Phys.* **41** (1993) 307 [arXiv:0709.1075] [INSPIRE].

[78] G. Colangelo, M. Hoferichter, M. Procura and P. Stoffer, *Dispersion relation for hadronic light-by-light scattering: theoretical foundations*, *JHEP* **09** (2015) 074 [arXiv:1506.01386] [INSPIRE].

JHEP08(2022)295

[79] R. García-Martín and B. Moussallam, *MO analysis of the high statistics Belle results on $\gamma\gamma \to \pi^+\pi^-$, $\pi^0\pi^0$ with chiral constraints*, *Eur. Phys. J. C* **70** (2010) 155 [arXiv:1006.5373] [INSPIRE].

[80] M. Hoferichter, D.R. Phillips and C. Schat, *Roy-Steiner equations for $\gamma\gamma \to \pi\pi$*, *Eur. Phys. J. C* **71** (2011) 1743 [arXiv:1106.4147] [INSPIRE].

[81] B. Moussallam, *Unified dispersive approach to real and virtual photon-photon scattering at low energy*, *Eur. Phys. J. C* **73** (2013) 2539 [arXiv:1305.3143] [INSPIRE].

[82] I. Danilkin and M. Vanderhaeghen, *Dispersive analysis of the $\gamma\gamma^* \to \pi\pi$ process*, *Phys. Lett. B* **789** (2019) 366 [arXiv:1810.03669] [INSPIRE].

[83] M. Hoferichter and P. Stoffer, *Dispersion relations for $\gamma^*\gamma^* \to \pi\pi$: helicity amplitudes, subtractions, and anomalous thresholds*, *JHEP* **07** (2019) 073 [arXiv:1905.13198] [INSPIRE].

[84] I. Danilkin, O. Deineka and M. Vanderhaeghen, *Dispersive analysis of the $\gamma^*\gamma^* \to \pi\pi$ process*, *Phys. Rev. D* **101** (2020) 054008 [arXiv:1909.04158] [INSPIRE].

[85] S.P. Schneider, B. Kubis and F. Niecknig, *The $\omega \to \pi^0\gamma^*$ and $\phi \to \pi^0\gamma^*$ transition form factors in dispersion theory*, *Phys. Rev. D* **86** (2012) 054013 [arXiv:1206.3098] [INSPIRE].

[86] BELLE collaboration, *High-Statistics Study of the $\tau^- \to \pi^-\pi^0\nu_\tau$ Decay*, *Phys. Rev. D* **78** (2008) 072006 [arXiv:0805.3773] [INSPIRE].

JHEP08(2022)295